Scientific
Research

Synthesis and Electrical Analysis of Ba$_5$GdTi$_3$V$_7$O$_{30}$ Ceramics

Bana B. Mohanty[1], Priyadarshini S. Sahoo[1*], Mahapatra P. K. Sahoo[2], Ram N. P. Choudhary[3]

[1]Department of Physics, Betnoti College Betnoti, Mayurbhanj, India; [2]Department of Physics, RGU-IIIT, Krishna, India; [3]Department of Physics, ITER, Bhubaneswar, India.
Email: [*]ps_rilly@yahoo.com

ABSTRACT

A polycrystalline sample of Ba$_5$GdTi$_3$V$_7$O$_{30}$ was prepared using a mixed oxide method at high temperature (*i.e.*, at 950˚C). The formation of single-phase compound with orthorhombic structure at room temperature was confirmed from preliminary X-ray diffraction study. Detailed studies of dielectric properties of Ba$_5$GdTi$_3$V$_7$O$_{30}$, investigated in a wide frequency range (10^2 - 10^6 Hz) at different temperatures (33˚C - 500˚C) showed that these properties of the material are strongly dependent on frequency and temperature. The existence a dielectric anomaly suggests that the compound has a transition temperature at ~385˚C. The nature of the variation of conductivity and value of activation energy in different regions, calculated from the temperature dependence of ac conductivity (dielectric data) suggest that the conduction process is of mixed type (*i.e.*, ionic-polaronic and space charge generated from the oxygen ion vacancies). The ac conductivity spectrum obeys Jonscher's universal power law.

1. Introduction

Though a large number of ferroelectric oxides of different structural families (*i.e.*, perovskite, tungsten-bronze, spinel, etc.) are now available, some compounds of perovskite and tungsten-bronze (TB) families [1-3] in pure and/or complex form, such as BaTiO$_3$, LiNbO$_3$, PbTiO$_3$, Pb(ZrTi)O$_3$, barium sodium niobate, potassium lanthanum niobate etc., have been found to be important because of their various physical properties suitable for device applications. Many ferroelectric compounds with tungsten-bronze structure have been widely investigated and found application particularly in devices such as transducers, actuators, capacitors, and nonvolatile ferroelectric random access memory because of their interesting ferroelectric, pyroelectric, piezoelectric, and nonlinear optic properties [4-8]. The tungsten-bronze structure consists of a complex array of distorted BO$_6$ octahedra sharing corners in such a way that three different types of interstices (A, B and C) are available for cation occupying in the general formula (A$_1$)$_2$(A$_2$)$_4$(C)$_4$(B$_1$)$_2$(B$_2$)$_8$O$_{30}$. Generally, the smallest interstice C is empty, so the general formula is A$_6$B$_{10}$O$_{30}$ for the filled tungsten-bronze structure. Nowadays, the research of lead-free electroceramics and their applications are extremely important as a result of implementing the strategy for the sustainable development of the world, and strengthening to the consciousness of environmental protection. Detailed literature survey shows that though a lot of work has been done on TB structured compounds [9-14]. In view of the importance of the eco-friendly (lead-free) materials of the above family, we have recently carried out the systematic structural and electrical studies of the Ba$_5$GdTi$_3$V$_7$O$_{30}$ compound.

2. Experimental Procedure

Polycrystalline sample of Ba$_5$GdTi$_3$V$_7$O$_{30}$ (BGTV) was prepared using high temperature solid-state reaction techniques. The stoichiometric mixtures of the high purity (99.9%) powders of BaCO$_3$ (M/s Sarabhai M. Chemicals Pvt. Ltd., India), SrCO$_3$ (M/s Sarabhai M. Chemicals Pvt. Ltd., India), TiO$_2$ (M/s Sarabhai M. Chemicals Pvt. Ltd., India), Sm$_2$O$_3$ (M/s Sarabhai M. Chemicals Pvt. Ltd., India), and V$_2$O$_5$ (M/s. Koch Light Ltd., England) were weighed and thoroughly ground in an agate mortar to obtain homogeneous mixtures and calcined at 950˚C for 12 hrs. The calcined powders were grounded and dried, followed by mixing with organic binder polyvinyl alcohol (PVA) to prepare cylindrical pellets of 10 mm diameter and 1 - 2 mm thickness at the pressure of 4×10^6 N/m^2. The pellets were sintered in air at 1000˚C for 12 h to yield dense ceramics. The binder was burnt out during

high temperature sintering. The formation and quality of the compound was checked by an X-ray diffraction (XRD) technique. The X-ray diffraction pattern of the compounds was recorded at room temperature using an X-ray powder diffractometer (Rigaku, Miniflex) with CuK_α radiation (λ = 1.5405 Å) in a wide range of Bragg's angles 2θ ($20° \leq 2\theta \leq 80°$) with a scanning rate of 3°/minute. To study the surface morphology of the sintered pellets, both the surfaces were made flat and parallel. On the flat and clean surface gold coating was done by a sputtering method to increase the resolution of micrograph. Microstructures of sintered pellets were recorded by JEOL-JSM: 5800 model scanning electron microscope (SEM). The average grain size was determined by a linear intercept method. The electrical properties of the sintered pellets were studied with the data recorded by an impedance analyzer (HIOKI LCR Hi tester LCR meter (Model: 3532)) over a wide frequency range (10^2 - 10^6 Hz) at different temperatures (31°C - 500°C). The hysteresis loops (P-E Loop) of the poled samples (6 kV/cm for 24 hours in the silicon oil) were obtained at room temperature using precision material analyzer (M/S. Radiant Technologies Inc., NM and USA) integrated with 4 kV voltage amplifiers.

3. Results and Discussion

3.1. Structural and Microstructural Studies

The room temperature XRD pattern (**Figure 1**) of the calcined powder, which is different from those of the ingredients (JCPDS file nos. 22-1141, 02-0364 and 75-0457), shows the formation of a single phase new compound. All the reflection peaks of the pattern are indexed in tetragonal or orthorhombic crystal system and in different cell configurations using software "POWD" [15].

Since TB compounds have tetragonal or orthorhombic crystal structure out of which an orthorhombic unit cell was selected on the basis of the best agreement between observed and calculated interplaner spacing d (*i.e.*, $\Sigma\Delta d$ = $d_{obs} - d_{cal}$ = minimum). Then the selected lattice parameters are refined using the least-squares method, which are found to be a = 4.3691 (7) Å, b = 18.8181 (7) Å, c = 13.5254 (7) Å and volume V = 1112.05 $Å^3$ for the compound (the number in parenthesis is estimated standard deviation of lattice parameters).

The unit cell parameters are consistent, and are in good agreement, with those reported earlier [9,16,17] for TB structural family. Unfortunately, it is not possible to determine the space group of the compound with the limited powder data. The crystallite size (P) of BDTV was roughly estimated from the broadening of a few XRD peaks (in wide 2θ range) using the Scherrer's equation [18]: P = $K\lambda/(\beta_{1/2} \cos \theta_{hkl})$ (where K = constant = 0.89, λ = 1.5405 Å and $\beta_{1/2}$ = peak width of the reflection at half intensity). The average value of P was found to be 12 nm. The effects of strain, instrument and other defects on broadening are ignored in the calculation.

The SEM micrograph of the compounds with different magnifications at room temperature is shown in **Figure 1** (inset). It is found that the grains are inhomogeneously and uniformly distributed over the entire surface of samples. The grain size evaluated from histogram is found to be in the range of 1.6 µm. A similar type of microstructure was found in many materials of this family [16,17].

3.2. Dielectric Study

Temperature dependence of dielectric constant (ε_r) for BGTV is shown in **Figure 2(a)**. The value of relative dielectric constant (ε_r) initially increases with increase in
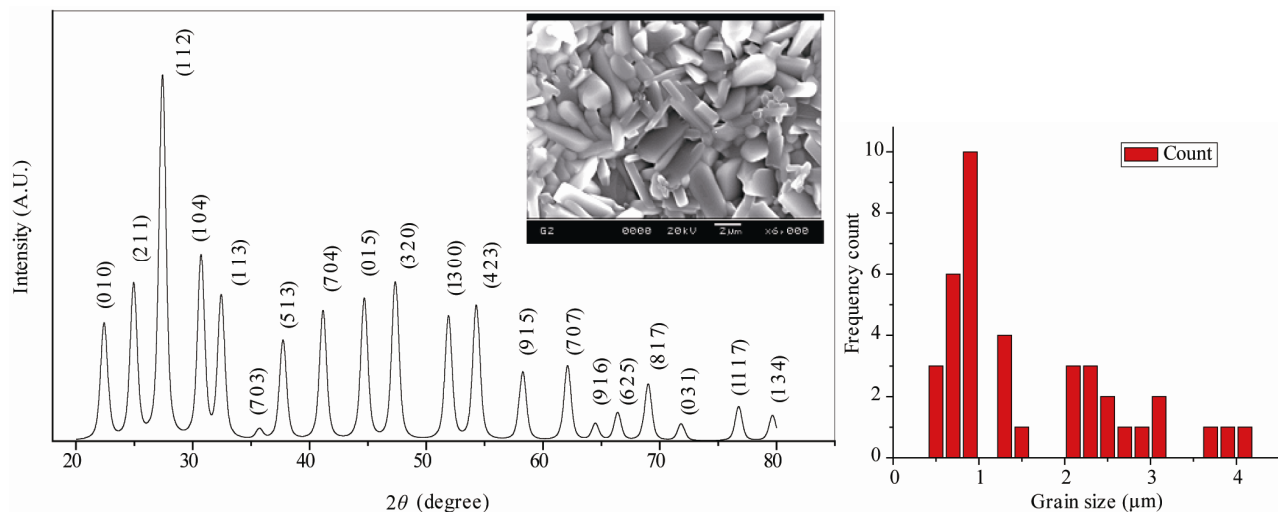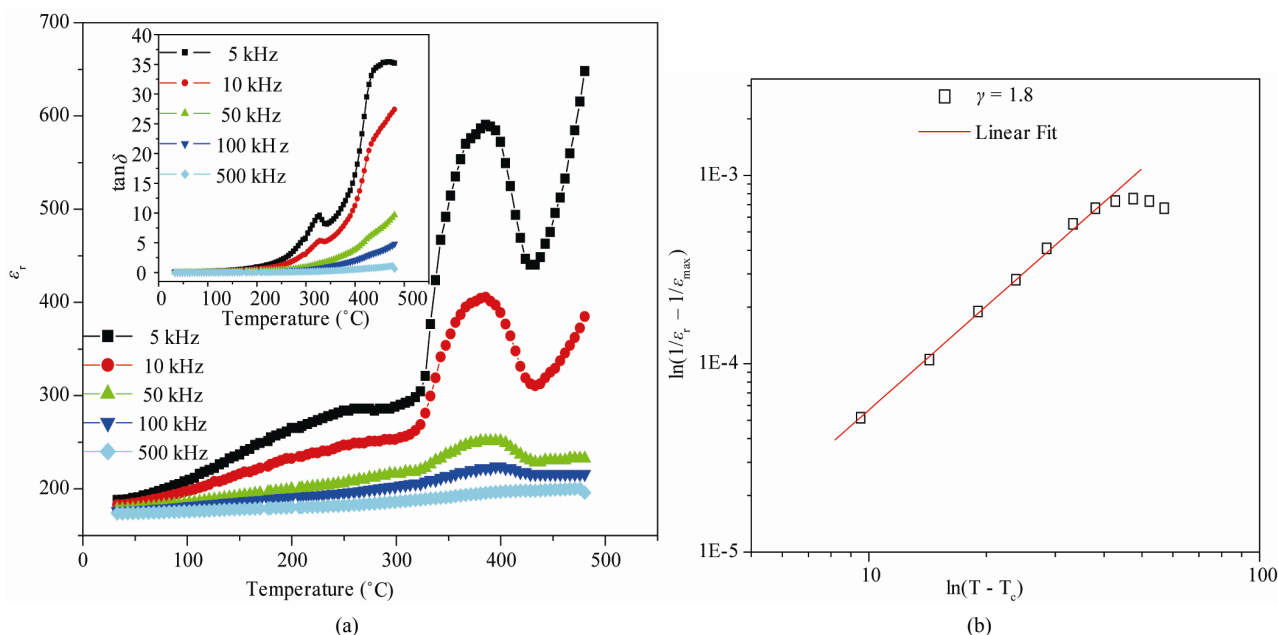

Figure 1. Room temperature XRD and SEM micrograph (inset) and histograms (right) showing the grain size distribution of $Ba_5GdTi_3V_7O_{30}$.

Figure 2. (a) Temperature variation of relative dielectric constant (ε_r), loss tangent (tanδ) (inset) at 5 - 500 kHz and (b) diffusivity graph of Ba$_5$GdTi$_3$V$_7$O$_{30}$.

temperature, reaches to a maximum (peak) value at transition temperature (T$_c$ ~386°C), and then decreases and on farther increasing the temperature, the ε_r value increases. In our previous study using the same material, no expected dielectric anomaly was observed within the measured temperature range (30°C - 500°C) when Sm was doped in place of Gd, where as for Dy doped compound the transition temperature was ~430°C [19,20]. Also it is observed that the values of tanδ (**Figure 2(a)** (inset)) increase with increase in temperature which may be due to space charge polarization. The low value of tanδ represents the good quality of ferroelectric material under observation. At low temperature the change in the values of tanδ of the compound is found considerably small. It then increases significantly at high temperatures. This may be due to enhanced conductivity in this compound, and also the reduction in ferroelectric domain wall's contribution at high temperatures (paraelectric phase) [15, 16]. Ferroelectric-paraelectric phase transition was confirmed by appearance of hysteresis loops (as shown in the later section).

The broadening of dielectric peak indicates the existence of diffuse phase transition. The degree of disorder or diffusivity (γ) of the compound is estimated by an empirical relation; $\ln(1/\varepsilon_r - 1/\varepsilon_{max}) = \gamma \ln(T - T_C) + \ln K$ where T is the temperature and K is a constant. The value of γ at different frequency, calculated from the slope, is given in **Figure 3**. Generally, the value of γ is between 1 (for normal ferroelectrics) and 2 (for completely disordered system). The above value of γ ($1 \leq \gamma \leq 2$) shows a deviation from normal ferroelectric behavior, which in-

dicates the occurrence of disordering in the system [17]. Kenzig [21,22] showed that when the paraelectric phase of BaTiO$_3$ transform to the ferroelectric macro domain phase, small domains of about 100 Å are formed in a temperature range of about 1°C (above T$_c$). They constitute the nucleation of the low temperature ferroelectric phase. Diffuse phase transition occurs due to fluctuation or substitutional disorder in the arrangement of cations at different crystallographic sites which is found in most of the niobate compounds of TB family.

3.3. Hysterisis Study

Figure 3 shows the variation of polarization as a function of electric field on poled sample at room temperature.
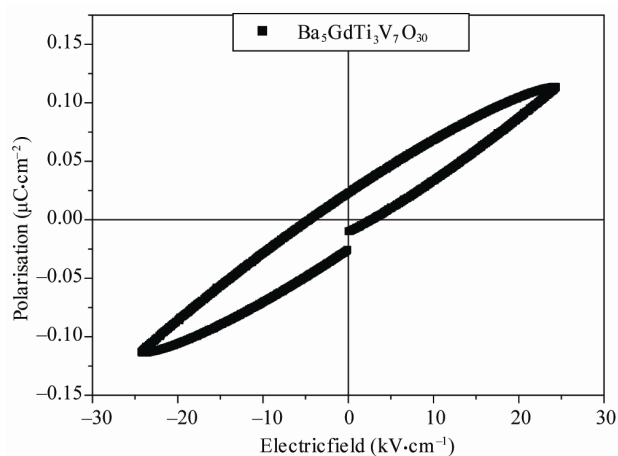
Figure 3. Room temperature P-E loop of Ba$_5$GdTi$_3$V$_7$O$_{30}$.

The appearance of hysteresis loop confirms the assumption of ferroelectric-paraelectric phase transition. Remanant polarization was found to be 2Pr = 0.0539 μC/cm² at an applied electric field of and 5.6 kV/cm, respectively. A proper hysteresis loop is not obtained because of the lossy characteristics of the material.

3.4. Conductivity Study

The ac electrical conductivity (σ_{ac}) is calculated using the dielectric data and an empirical relation. $\sigma_{ac} = \omega \varepsilon_r \varepsilon_0 \tan\delta$, where ε_0 = permittivity of free space and ω = angular frequency. **Figure 4** shows frequency dependence of ac conductivity (σ_{ac}) at various temperatures. At low frequencies and high temperatures, we observe plateaus of σ_{ac} (*i.e.* frequency independent values of conductivity) which corresponds to the dc conductivity. The observed frequency dependent conductivity found to obey Jonscher's universal power law: $\sigma(\omega) = \sigma_{dc} + A\omega^n$ where n is the frequency exponent with $0 < n < 1$ (**Table 1**) and A is the temperature dependent pre-exponential factor [23].

In pure and stoichiometric state of the compounds, the V ions are in the 5+ valence states and should behave as an insulator with very low dielectric losses. But oxygen vacancies and charge carriers (electrons and holes) are generated during the calcinations and sintering processes, thus contributing to a complex system of conduction mechanisms. **Figure 5** shows the variation of σ_{ac} as a function of temperature at different frequencies. The nature of the variation is almost linear over a wide temperature region obeying the Arrhenius relation: $\sigma_{ac} = \sigma_0$ $\exp(-E_a/k_BT)$, where the symbols have their usual meanings. **Figure 5** has two distinct regions: one in high and other in low temperature regions named as: I and II for both the frequencies. The values of activation energy (E_a) of the compound are calculated using the above equation. The variation in slope in these regions indicates the presence of different conduction mechanisms and hence, has different values of activation energy (0.22 eV and 0.17 eV in region I and 0.54 eV and 0.48 eV in region II at 10, 100 kHz respectively). The merging of two curves at higher temperature region indicates the occurrence of frequency independent dc conduction. These low values of activation energy suggest that a small amount of energy is required to activate the carriers/electrons for elec-

Table 1. Value of frequency exponent n with temperature obtained from Jonscher's universal power law fitting.

Serial no.	Temperature in ˚C	n
1	30	0.61
2	50	0.55
3	100	0.53
4	150	0.45
5	200	0.44
6	250	0.47
7	300	0.55
8	350	0.29
9	400	0.29
10	450	0.19
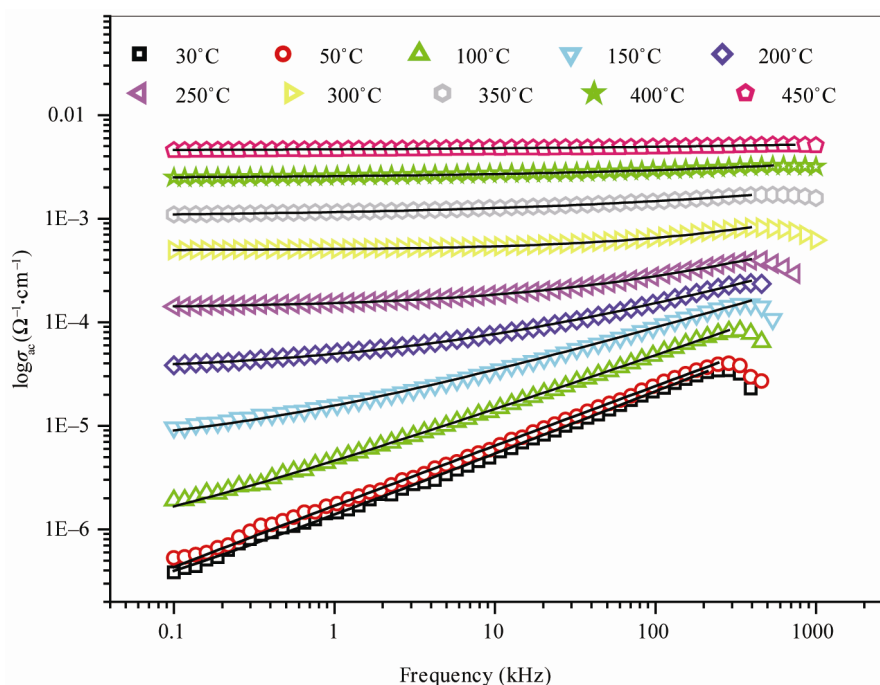
Figure 4. Variation of σ_{ac} with frequency of $Ba_5GdTi_3V_7O_{30}$.
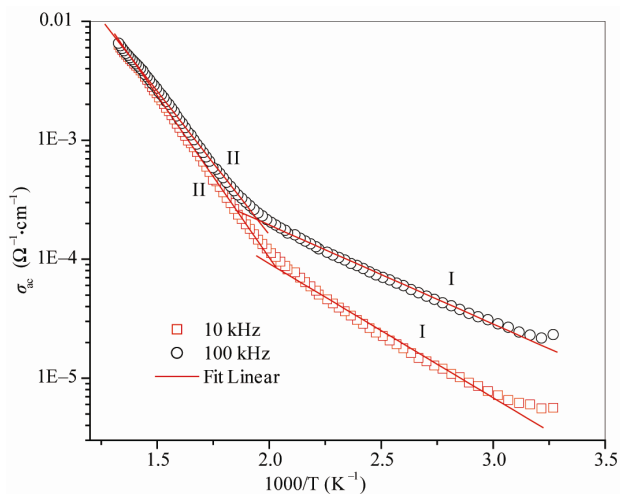
Figure 5. Variation of σ$_{ac}$ with inverse temperature of Ba$_5$GdTi$_3$V$_7$O$_{30}$.

trical conduction. Increases of σ_{ac} with temperature may be due to oxygen ion vacancies (loss of oxygen created during sintering) and the charge compensation.

4. Conclusion

According to the experimental results obtained, the poly-crystalline compound BGTV, formed by high-temperature solid-state reaction technique, is characterized to be single phase with orthorhombic structure at room temperature and undergoes ferroelectric-paraelectric phase transitions at around 386°C. The comparatively low room temperature dielectric constant indicates that these materials may have attractive benefits in electrooptic and infrared pyroelectric detector applications when grown in bulk single crystal or thin-film form. The ac conductivity spectrum was found to obey Jonscher's universal power law. The activation energy of the compound was found to be different in different region indicating presence of different conduction mechanism.

5 Acknowledgements

REFERENCES

[1]   L. X. Zhang, W. Chen and X. Ren, "Large Recoverable Electrostrain in Mn-Doped (Ba,Sr) TiO$_3$ Ceramics," *Applied Physics Letters*, Vol. 85, No. 23, 2004, pp. 5658-5660. doi:10.1063/1.1829394

[2]   W. L. She, K. K. Lee and W. K. Lee, "All Optical Quasi-Steady-State Photorefractive Spatial Solitons," *Physical Re-view Letters*, Vol. 85, No. 12, 2000, pp. 2498-2501. doi:10.1103/PhysRevLett.85.2498

[3]   M. E. Lines and A. M. Glass, "Principles and Applications of Ferroelectric and Related Materials," Clarendon Press, Oxford, 1977.

[4]   B. Jaffe, W. R. Cook and H. Jaffe, "Piezoelectric Ceramics," Academic Press, London, 1971.

[5]   K. Uchino, "Piezoelectric Actuators and Ultrasonic Motors," Kluwer Academics, Boston, 1997.

[6]   R. R. Neurgaonkar, M. H. Kalisher, T. C. Lim, E. J. Staples and K. L. Keester, "Czochralski Single Crystal Growth of Sr$_{.61}$Ba$_{.39}$Nb$_2$O$_6$ for Surface Acoustic Wave Applications," *Materials Research Bulletin*, Vol. 15, No. 9, 1980, pp. 1235-1240. doi:10.1016/0025-5408(80)90025-2

[7]   W. Sakamoto, Y.-S. Horie, T. Yogo and S.-I. Hirano, "Synthesis and Properties of Highly Oriented (Sr, Ba)(Nb, Ta)$_2$O$_6$ Thin Films by Chemical Solution Deposition," *Japanese Journal of Applied Phys- ics*, Vol. 40, 2001, pp. 5599-5604. doi:10.1143/JJAP.40.5599

[8]   P. Ganguly and A. K. Jha, "Investigations of Dielectric, Pyroelectric and Electrical Properties of Ba$_5$SmTi$_3$Nb$_7$O$_{30}$ Ferroelectric Ceramic," *Journal of Alloys and Compounds*, Vol. 484, No. 1-2, 2009, pp. 40-44. doi:10.1016/j.jallcom.2009.05.034

[9]   M. R. Ranga Raju, R. N. P. Choudhary and S. Ram, "Dielectric and Electrical Properties of Sr$_5$EuCr$_3$Nb$_7$O$_{30}$ Nanoceramics Prepared Using a Novel Chemical Route," *Physica Status Solidi* (*b*), Vol. 239, No. 2, 2003, pp. 480-489. doi:10.1002/pssb.200301832

[10] P. V. Bijumon, V. Kohli, Om Parkash, M. R. Varma and M. T. Sebastian, "Dielectric Properties of Ba$_5$MTi$_3$A$_7$O$_{30}$ [M = Ce, Pr, Nd, Sm, Gd, Dy and Bi; A = Nb, Ta] Ceramics," *Materials Science and Engineering*: *B*, Vol. 113, No. 1, 2004, pp. 13-18. doi:10.1016/j.mseb.2004.05.023

[11] M. R. Ranga Raju and R. N. P. Choudhary, "Structural, Dielectric and Electrical Properties of Sr$_5$RTi$_3$Nb$_7$O$_{30}$ (R = Gd and Dy) Ceramics," *Materials Letters*, Vol. 57, No. 19, 2003, pp. 2980-2987. doi:10.1016/S0167-577X(02)01408-8

[12] H. Zhang, Z. Q. Liu, C. L. Diao R. Z. Yuan and L. Fang, "Structural and Dielectric Properties of Sr$_4$Ln$_2$Ti$_4$Ta$_6$O$_{30}$ (Ln = Nd and Sm) Ceramics," *Materials Letters*, Vol. 59, No. 21, 2005, pp. 2634-2637. doi:10.1016/j.matlet.2005.04.006

[13] X. H. Zheng and X. H. Zhou, "Crystal Structure and Dielectric Properties of La^{3+} Substituted Ba$_5$LaTi$_3$Ta$_7$O$_{30}$ Ceramics," *Journal of Materials Science*: *Materials in Electronics*, Vol. 17, No. 12, 2006, pp. 987-991. doi:10.1007/s10854-006-9007-5

[14] L. Fang, H. Zhang, J. F. Yang, X. K. Hong and F. C. Meng, "Preparation, Characterization and Dielectric Properties of Sr$_5$LnTi$_3$Ta$_7$O$_{30}$ (Ln = La, Nd) Ceramics," *Journal of Materials Science*: *Materials in Electronics*, Vol. 15, No. 6, 2004, pp. 355-357. doi:10.1023/B:JMSE.0000025677.53710.c8

[15] E. Wu, POWD, An Interactive Powder Diffraction Data Interpretation and Indexing Program, Version 2.1 (School

of Physical Sciences, Flinders University South Bedford Park), SA 5042 Australia.

[16] P. S. Sahoo, A. Panigrahi, S. K. Patri and R. N. P. Choudhary, "Structural, Dielectric, Electrical and Piezoelectric Properties of $Ba_4SrRTi_3V_7O_{30}$ (R = Sm, Dy) Ceramics," *Central European Journal of Physics*, Vol. 6, No. 4, 2008, pp. 843-848. doi:10.2478/s11534-008-0112-3

[17] P. S. Sahoo, A. Panigrahi, S. K. Patri and R. N. P. Choudhary, "Ferroelectric Phase Transition in $Ba_4SrSmTi_3V_7O_{30}$ Ceramics," *Materials Letters*, Vol. 63, No. 11, 2009, pp. 864-866. doi:10.1016/j.matlet.2009.01.053

[18] H. P. Klug and L. E. Alexander, "X-Ray Diffraction Procedures for Polycrystalline and Amorphous Materials," Willey-Interscience, New York, 1974.

[19] P. S. Sahoo, A. Panigrahi, S. K. Patri and R. N. P. Choudhary, "Structural and Impedance Properties of $Ba_5DyTi_3V_7O_{30}$," *Journal of Materials Science*: *Materials in Electronics*, Vol. 20, No. 6, 2009, pp. 565-569. doi:10.1007/s10854-008-9766-2

[20] P. S. Sahoo, A. Panigrahi, S. K. Patri and R. N. P. Choudhary, "Structural and Electrical Properties of $Ba_5SmTi_3V_7O_{30}$ Ceramics," *Journal of Materials Science*: *Materials in Electronics*, Vol. 21, No. 1, 2010, pp. 160-167. doi:10.1007/s10854-009-9887-2

[21] R. Clarke and D. Siapkas, "Temperature-Dependent Raman Spectra of Ferroelectric Potassium Strontium Niobate," *Journal of Physics C*: *Solid State Physics*, Vol. 8, No. 3, 1975, pp. 377-379. doi:10.1088/0022-3719/8/3/016

[22] R. Williams, "Surface Layer and Decay of the Switching Properties of Barium Titanate," *Journal of Physics and Chemistry of Solids*, Vol. 26, No. 2, 1965, pp. 399-405. doi:10.1016/0022-3697(65)90169-1

[23] A. S. Bhalla, R. Guo, L. E. Cross, G. Burns, F. H. Dacol, and R. R. Neurgaonkar, "Glassy Polarization in the Ferroelectric Tungsten Bronze (Ba, Sr)Nb_2O_6," *Journal of Applied Physics*, Vol. 71, No. 11, 1992, pp. 5591-5595. doi:10.1063/1.350537